Contribution from the Department of Chemistry,
University of Wisconsin—Madison, Madison, Wisconsin 53706

Structural Characterization of $[AsPh_4]^+[Fe_4(NO)_7(\mu_3\text{-}S)_3]^-$. Stereochemical and Bonding Relationship of the Roussin Black Monoanion with the Red Ethyl Ester, $Fe_2(NO)_4(\mu_2\text{-}SC_2H_5)_2$, and $Fe_4(NO)_4(\mu_3\text{-}S)_4$

CYNTHIA TING-WAH CHU and LAWRENCE F. DAHL*

Received April 7, 1977 AIC70257V

The classical black Roussin monoanion, $[Fe_4(NO)_7(\mu_3\text{-}S)_3]^-$, was produced unexpectedly by a Na/Hg amalgam reduction of $Fe_4(NO)_4(\mu_3\text{-}S)_4$. An x-ray diffraction analysis of its tetraphenylarsonium salt showed the monoanion to be comprised of a trigonal pyramid of four iron atoms with triply bridging sulfur atoms and Fe–Fe electron-pair bonds linking the apical Fe(NO) fragment to each of the three basal $Fe(NO)_2$ moieties. A high-resolution infrared spectrum (KBr) pellet of the nitrosyl stretching region showed a remarkable similarity with that previously reported for the hydrated ammonium salt and thereby provided strong evidence for a close geometrical resemblance of the monoanion in the two salts. The distances and bond angles of the Fe_4S_3 fragment were found to agree within experimental error with those in the structure of $Cs[Fe_4(NO)_7(\mu_3\text{-}S)_3]\cdot H_2O$ determined by Johansson and Lipscomb from x-ray photographic measurements in 1958. The much more precisely determined geometry obtained from the present diffractometry measurements has allowed the formulation of a qualitative metal cluster bonding model based upon a close compliance of the dimensions of the black monoanion with those of the corresponding fragments in the red Roussin $Fe_2(NO)_4(\mu_2\text{-}SC_2H_5)_2$ and the cubane-like $Fe_4(NO)_4(\mu_3\text{-}S)_4$ molecules. Two tetraphenylarsonium cations and two monoanions crystallize in a centrosymmetric primitive triclinic cell with a = 13.018 (3) Å, b = 13.905 (4) Å, c = 9.800 (2) Å, α = 98.47 (2)°, β = 97.98 (2)°, γ = 72.12 (2)°, and V = 1661.4 (7) Å^3. Least-squares refinement yielded R_1 = 4.5% and R_2 = 4.9% for 2148 independent diffractometry-collected data with $I \geq 2\sigma(I)$.

Introduction

This investigation was an outgrowth of an electrochemical study[1,2] of the redox properties of the neutral $Fe_4(NO)_4(\mu_3\text{-}S)_4$ molecule which possesses cubic T_d symmetry with the Fe_4S_4 core containing a completely bonding iron tetrahedron. A cyclic voltammogram showed two reversible, one-electron waves indicating the existence of a reduced monoanion (n = −1) as well as an oxidized monocation (n = +1). The preparation and crystallographic characterization of the monoanion was of particular interest in that it provides an operational test of a qualitative molecular orbital cluster model[3] utilized[1,2] to describe the bonding and to differentiate the electronic configurations of $Fe_4(NO)_4(\mu_3\text{-}S)_4$, $[Fe_4(\eta^5\text{-}C_5H_5)_4(\mu_3\text{-}S)_4]^n$ (n = 0,[4] +1,[5] +2[6]), and the $[Fe_4(SR)_4(\mu_3\text{-}S)_4]^n$ anions (n = −1, −2, −3)[7] from one another. This LCAO–MO scheme,[3] which correlates geometries to electronic configurations, suggests that a one-electron reduction of the parent $Fe_4(NO)_4(\mu_3\text{-}S)_4$ molecule to the monoanion would involve the addition of an electron to a triply degenerate antibonding metal cluster orbital which then would be expected to produce via a first-order Jahn–Teller distortion a tetragonal D_{2d} geometry with a relative lengthening of either two or four of the six Fe–Fe distances.

A chemical reduction of the neutral compound by cobaltocene to give $[Co(\eta^5\text{-}C_5H_5)_2]^+[Fe_4(NO)_4(\mu_3\text{-}S)_4]^-$ was carried out, but unfortunately an x-ray diffraction examination of the isolated crystals failed to yield the detailed structure due to a complicated crystal disorder and/or crystal twinning.[1]

Subsequent reductions of $Fe_4(NO)_4(\mu_3\text{-}S)_4$ were performed with Na/Hg amalgam in THF at room temperature. After a number of unsuccessful attempts to obtain crystals of the monoanion with either tetraphenylarsonium or bis(triphenylphosphine)iminium counterions by use of various crystallization procedures, suitable crystals for x-ray diffraction analysis were finally obtained from a solvent diffusion technique. Unfortunately, the monoanion of the isolated tetraphenylarsonium salt was unexpectedly shown from the structural determination to be the classical Roussin black $[Fe_4(NO)_7(\mu_3\text{-}S)_3]^-$ monoanion whose geometry had been previously elucidated from an early x-ray diffraction photographic study of a monohydrated cesium salt by Johansson and Lipscomb[8] in 1958. Since our results stem from diffractometry data and thereby represent a much higher degree of precision, the work given here has offered the opportunity to compare the structural features of the $[Fe_4(NO)_7(\mu_3\text{-}S)_3]^-$ monoanion with those of related compounds and to evaluate further the nature of bonding in this complex.

The Roussin monoanion presumably is formed as a decomposition product from the $[Fe_4(NO)_4(\mu_3\text{-}S)_4]^-$ monoanion during the acetone extraction and/or subsequent slow recrystallization from a methylene chloride–heptane mixture.

Experimental Section

Preparation. All reductions were performed under argon in Schlenk-type apparatus which was cleaned by standard chromic acid solution and then dried at 120 °C. THF (Mallinckrodt Chemical Works) was refluxed over sodium benzophenone before distillation. Methylene chloride (Aldrich Chemical Co., Inc.) was distilled over phosphorus pentoxide. Heptane (Mallinckrodt Chemical Works) was used without further purification. The procedure of King[9] was utilized to prepare Na/Hg amalgams.

In one reaction a 150-mL THF solution containing 0.2 g (0.4 mmol) of $Fe_4(NO)_4(\mu_3\text{-}S)_4$ was added dropwise over a 30-min period into a Na/Hg amalgam (2.3 mL of Hg to 0.3 g of Na) suspended in 50 mL of THF. After 5 min of stirring under N_2, the solution was filtered several times to get rid of the grayish fine powder. A 50-mL acetone solution containing 0.2 g (~0.4 mmol) of $(C_6H_5)_4AsCl$ was added and the mixture stirred overnight under a N_2 atmosphere. After removal of the solvent under vacuum, the residue was washed first with hexane and then with toluene to separate the insoluble ionic product from the soluble neutral species. The precipitate was extracted with THF and then with acetone. The THF extract decomposed during recrystallization. The acetone extract was dried under vacuum, and the product was separated into two portions for recrystallization by solvent diffusion from a CH_2Cl_2–heptane mixture and from an acetone–ether mixture under argon. Black crystals suitable for x-ray diffraction measurements were obtained over a 1-week period from both solutions. The crystallographic and infrared results presented here are from the crystalline sample obtained from the CH_2Cl_2–heptane mixture.[10]

A low-resolution infrared spectrum (Beckman IR-8) in CH_2Cl_2 solution exhibited a broad band in the terminal nitrosyl stretching region at ca. 1725 cm^{-1}. A subsequent high-resolution infrared spectrum (Digilab FTS-20 Fourier transform spectrometer with 4.0-cm^{-1} resolution) in the solid state (KBr pellet), performed after the crystals were determined from the x-ray diffraction analysis to

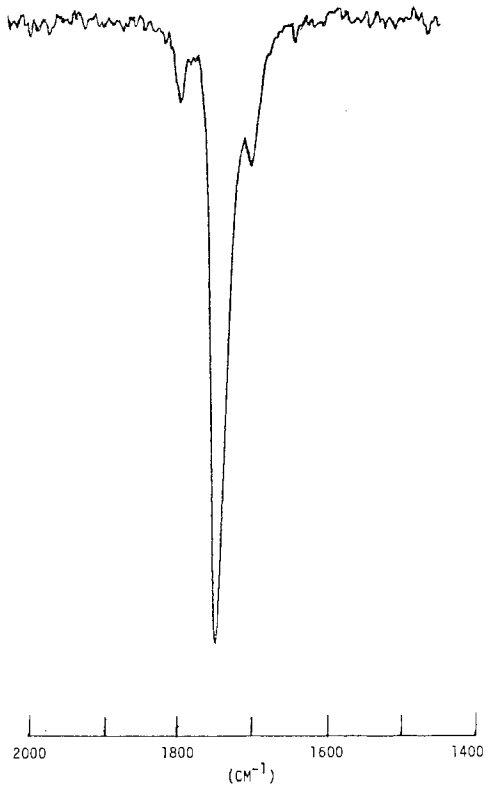

Figure 1. Solid-state infrared spectrum (KBr pellet) of $[AsPh_4]^+$-$[Fe_4(NO)_7(\mu_3\text{-}S)_3]^-$.

be $[AsPh_4]^+[Fe_4(NO)_7(\mu_3\text{-}S)_3]^-$, revealed a very strong band at 1745 cm^{-1} along with sharp weak bands at 1800 and 1708 cm^{-1} (Figure 1).

Single-Crystal Data Collection. A black parallelepiped-shaped crystal of dimensions 0.28 × 0.28 × 0.12 mm in the directions perpendicular to the opposite parallel faces was used to collect the intensity data. The crystal was glued with epoxy cement to the end of a glass fiber which was sealed inside an argon-filled Lindemann glass capillary. Oscillation photographs indicated that the crystal possessed triclinic symmetry. This crystal was mounted and aligned on a Nova-automated Syntex $P\bar{1}$ diffractometer equipped with a scintillation counter, a pulse-height analyzer adjusted to admit 90% of the Mo K$\bar{\alpha}$ peak ($\lambda\alpha_1$ 0.709 26 Å, $\lambda\alpha_2$ = 0.713 54 Å), and a crystal-graphite monochromator set at a Bragg 2θ angle of 12.2°. Fifteen reflections were centered automatically and used in a least-squares refinement to determine the lattice constants and orientation matrix from which the settings for all data were generated. The θ–2θ scan technique was used with (stationary crystal)–(stationary counter) background counting at both extremes of each scan and with variable scan speeds ranging from 3.0 to 24.0°/min. The scan speeds and widths for individual diffraction maxima were determined by relative peak intensities, and the ratio of total background counting time to scan time was 0.667. Two standard reflections, periodically measured every 48 data reflections, showed no significant changes in their intensities during the entire data collection. Data were sampled once for four independent triclinic octants (viz., hkl, $\bar{h}kl$, $h\bar{k}l$, and $\bar{h}\bar{k}l$) for the range $3.0 \leq 2\theta \leq 40.0°$. Of the 3371 measured data, 2338 had intensities greater than $2\sigma(I)$ above background where $\sigma(I) = (S + B(t_s/t_b)^2 + EI^2)^{1/2}$ with S designating the scan count obtained in time t_s, B the total background count obtained in time t_b, E an empirical factor (0.0025), and I the integrated intensity equal to $S - B(t_s/t_b)$. After correction of the intensities for background and polarization of the incident beam due to the crystal monochromator,[11a] the data were merged[11b] to yield 3122 total unique reflections; the 2148 independent reflections with $I \geq 2\sigma(I)$ were used in the solution and refinement of the structure. An absorption correction[11c] was applied to the intensity data in that the calculated transmission coefficients (based on a linear absorption coefficient of 30.32 cm^{-1} for Mo Kα radiation)[12a] ranged from 0.45 to 0.68.

Unit Cell Data. The measured lattice constants for the triclinic cell at ca. 22° are a = 13.018 (3) Å, b = 13.905 (4) Å, c = 9.800 (2) Å, α = 98.47 (2)°, β = 97.98 (2)°, and γ = 72.12 (2)°. The unit cell volume is 1661.4 (7) $Å^3$. The total number of electrons per unit cell, $F(000)$, is 908. The observed density of 1.82 g/cm^3 measured by the flotation technique is in agreement with a calculated density of 1.84 g/cm^3 for Z = 2.

Structural Determination and Refinement. The possible space groups were either $P1$ or $P\bar{1}$; the structural determination and refinement were based upon centrosymmetric $P\bar{1}$ symmetry such that the crystallographically independent unit consists of one $[AsPh_4]^+$ cation and one monoanion. An analysis of the vectors from a computed three-dimensional Patterson map[11d] via PHASE[11e] yielded initial positions for one arsenic and four iron atoms, for which R_1 = 55.4%. Three sulfur, four nitrogen, and four oxygen atoms were subsequently located from a difference Fourier map (R_1 = 24.1%). It was realized at this time that the monoanion was not the desired cubane-like Fe_4S_4 nitrosyl monoanion but instead was the Roussin black $[Fe_4(NO)_7(\mu_3\text{-}S)_3]^-$ monoanion whose structure had been elucidated from an x-ray diffraction study by Johansson and Lipscomb[8] of a monohydrated cesium salt.

On the basis that the relatively precise x-ray diffractometry data would provide a more meaningful analysis of distances and angles in the monoanion than that obtained from the early x-ray photographic measurements of Johansson and Lipscomb,[8] it was decided to continue the present structural investigation. The remaining nonhydrogen atoms were located from successive difference Fourier syntheses (R_1 = 17%),[13] after which the hydrogen atoms for each of the four phenyl rings were fit to an idealized rigid-body group of D_{6h} symmetry with a C–H bond length of 1.0 Å.[11f] During all further refinements the coordinates of the hydrogen atoms were not varied but new idealized positions were recalculated from the changed carbon coordinates after every other least-squares cycle. Block-diagonal least-squares refinement[11g] of the nonhydrogen atoms with isotropic temperature factors converged after ten cycles at R_1 = 8.0% and R_2 = 10.7%.[13] Further block-diagonal least-squares refinement with anisotropic thermal parameters utilized for all nonhydrogen atoms except the phenyl carbons atoms converged at R_1 = 4.5% and R_2 = 4.9%. A final full-matrix least-squares cycle[11h] was performed in which only the coordinates of all nonhydrogen atoms were varied due to size limitations of the computer used. The final discrepancy indices for the 2148 independent reflections were R_1 = 4.5% and R_2 = 4.9%, while the standard deviation of an observation of unit weight (σ_1)[13] was 1.05. A difference Fourier map, which showed the largest peak to be less than 0.6 e/Å, revealed no anomalous features.[14-16]

The positional and thermal parameters from the output of the final full-matrix least-squares cycle are presented in Table I and interatomic distances and bond angles[11i] in Table II. Equations of the mean planes[11j] together with out-of-plane distances of atoms and dihedral angles between these planes are tabulated elsewhere along with the observed and calculated structure factors; see paragraph at end of paper regarding supplementary material.

Results and Discussion

General Description of the Crystal Structure. The solid-state structure of $[AsPh_4]^+[Fe_4(NO)_7(\mu_3\text{-}S)_3]^-$ consists of discrete cations and monoanions. Figure 2[11k] displays the configuration of the $[Fe_4(NO)_7(\mu_3\text{-}S)_3]^-$ monoanion whose overall architecture is essentially identical with that previously found by Johansson and Lipscomb[8] in the monohydrated cesium salt. The tetraphenylarsonium cation is found to possess normal As–C distances of range 1.90 (1)–1.91 (1) Å and an expected variation of tetrahedral C–As–C bond angles from 107.6 (4) to 111.8 (4)°. Table II shows that the isotropically refined carbon atoms in the four phenyl rings have a maximum spread of 0.04 Å about the observed mean value of 1.38 Å. Figure 3 gives a perspective view of the triclinic unit cell showing the arrangement of the two cations and two monoanions under $P\bar{1}$ symmetry. There is no evidence of unusual interionic interactions in that the shortest interionic nonhydrogen contacts exceed 3.0 Å with no CH···ON distances being less than 2.6 Å.

The $[Fe_4(NO)_7(\mu_3\text{-}S)_3]^-$ Monoanion. (a) Previously Determined Chemical and Physical Properties. Hydrated alkali metal salts of the black $[Fe_4(NO)_7(\mu_3\text{-}S)_3]^-$ monoanion as well

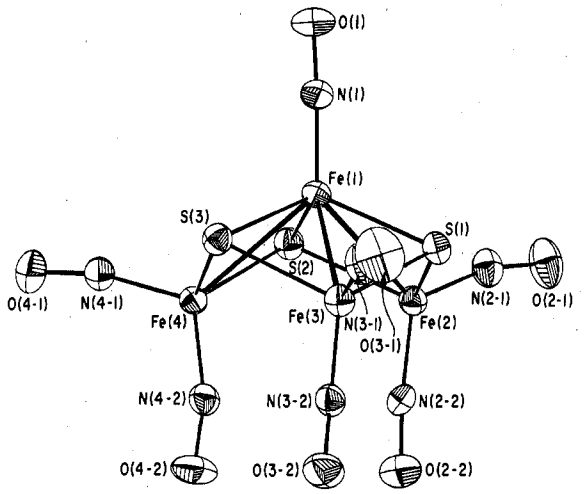

Figure 2. View of $[Fe_4(NO)_7(\mu_3\text{-}S)_3]^-$ monoanion (with 50% probability thermal ellipsoids) which has an idealized C_{3v} geometry with no crystallographically required symmetry. The apical Fe(1) is designated as Fe_A in the discussion, while the three chemically equivalent basal iron atoms (viz., Fe(2), Fe(3), and Fe(4)) are denoted as Fe_B.

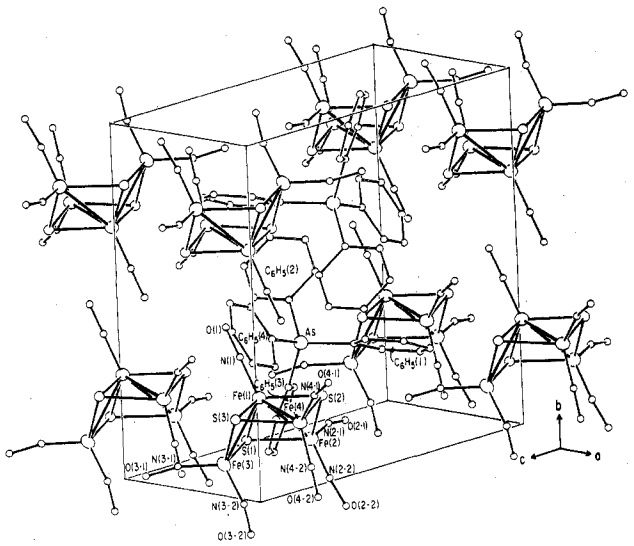

Figure 3. Perspective view of the triclinic unit cell of $[AsPh_4]^+$-$[Fe_4(NO)_7(\mu_3\text{-}S)_3]^-$ showing the arrangement of the two cations and two monoanions under $P\bar{1}$ symmetry.

as of the red $[Fe_2(NO)_4(\mu_2\text{-}S)_2]^{2-}$ dianion[17,18] were originally discovered by Roussin[19] in 1858, and their correct empirical formulas were first deduced in 1882 from elemental analyses by Pavel[20] who prepared $K[Fe_4(NO)_7(\mu_3\text{-}S)_3]\cdot H_2O$ from the reaction of $FeSO_4$ with $NaNO_2$ and KHS (H_2S + KOH). The black $K[Fe_4(NO)_7(\mu_3\text{-}S)_3]\cdot H_2O$ and red $K_2[Fe_2(NO)_4(\mu_2\text{-}S)_2]\cdot 4H_2O$ salts can conveniently be obtained[21] from the reaction of ferrous sulfide, nitric oxide, and potassium polysulfide, while the black potassium salt can be prepared from the red potassium salt by reaction with either iron nitrosyl sulfate[22] or aqueous carbon dioxide.[20a] It is noteworthy prior to the Johansson–Lipscomb crystallographic analysis[8] (which also showed that the cesium and potassium salts are isomorphous) that the constitution of the black salt was formulated by Manchot and Linckh[22] in 1926 as $\{[Fe(NO)_2\text{-}S]_3Fe(NO)\}K$ and that Seel[23] in 1942 proposed the correct overall geometry of the monoanion. A qualitative description of the electronic structure involving four nonbonding electrons on each iron and one electron pair in a highly delocalized molecular orbital among the four iron atoms was put forth by Johansson and Lipscomb[8] to account for the observed diamagnetism,[24] the high absorption coefficient, and the indicated differences in the Fe–N bond lengths for the two kinds of iron atoms.

Although Mössbauer data of the hydrated sodium salt were initially interpreted[25] to indicate only a single type of iron environment, a later, more detailed low-temperature investigation by Kostiner et al.[26] of the Mössbauer effect together with solution and solid-state infrared measurements of the corresponding ammonium salt established that the Mössbauer and infrared data support the crystallographically determined structure having two kinds of iron atoms in a 3:1 ratio and only terminal nitrosyl ligands.

(b) Structure and Properties; Comparison of Infrared and Crystallographic Data. The configuration[11k] of the $[Fe_4(NO)_7(\mu_3\text{-}S)_3]^-$ monoanion (Figure 2) is composed of a trigonal pyramid of four atoms with both triply bridging sulfur atoms and Fe–Fe electron-pair bonds linking the apical Fe(NO) fragment to each of the three basal $Fe(NO)_2$ moieties which are connected to one another by the three triply bridging sulfur atoms (but by no Fe–Fe bonds). The monoanion has an idealized C_{3v} geometry with no crystallographically required symmetry.

The three nitrosyl stretching frequencies obtained from a high-resolution infrared spectrum (KBr pellet) of $[AsPh_4]^+[Fe_4(NO)_7(\mu_3\text{-}S)_3]^-$ (Figure 1) are in remarkably close accord with those of $[NH_4]^+[Fe_4(NO)_7(\mu_3\text{-}S)_3]^-\cdot H_2O$ reported by Kostiner, Steger, and Rea[26] (viz., 1800 (vw) vs. 1800 (sh) cm^{-1}, 1745 (vs) vs. 1740 (vs) cm^{-1}, 1708 (sh) vs. 1710 (sh) cm^{-1}). These spectral data provide strong evidence for a close geometrical resemblance of the monoanion in the two salts. Group theoretical considerations based on C_{3v} symmetry lead to the prediction of five vibrational N–O stretching modes ($3A_1$ + 2E) which are all IR and Raman active. The relatively simple intensity pattern (with only three resolved frequencies) in the nitrosyl stretching region (Figure 1) precludes a tentative assignment of the bands.

The much greater precision of the $[AsPh_4]^+[Fe_4(NO)_7(\mu_3\text{-}S)_3]^-$ structure obtained from the x-ray diffractometry measurements is evidenced by the esd's of both the atomic coordinates and distances of the monoanion being three–five times lower than those of the corresponding atomic coordinates and distances of the monoanion in the $Cs[Fe_4(NO)_7(\mu_3\text{-}S)_3]\cdot H_2O$ structure determined[8] 20 years ago from x-ray photographic data. Nevertheless, the corresponding mean values of the distances and bond angles in the common monoanion of both structures show reasonably close agreement for the heavy-atom Fe_4S_3 fragment.

One prime structural feature which emerges from the present work concerns a bond-length reappraisal of the bonding interaction of the apical iron atom (denoted elsewhere[8] as Fe_I but here as Fe_A) to its lone nitrosyl ligand vs. the bonding interactions of the three basal iron atoms (designated elsewhere[8] as Fe_{II} but here as Fe_B) to their nitrosyl ligands.

In the $Cs[Fe_4(NO)_7(\mu_3\text{-}S)_3]\cdot H_2O$ structure, the mean of 1.67 Å for the six Fe_B–NO distances (of range 1.61 (4)–1.73 (4) Å) was regarded as a double-bond length whereas the shorter Fe_A–NO distance of 1.57 (4) Å was formulated as a triple-bond length.[8] This indicated bond-length trend (which was considered as perhaps not significant in view of the esd's) was cited by Johansson and Lipscomb[8] in support of their proposed valence electronic structure involving $Fe_A{\equiv}NO$ and $Fe_B{=}NO$ bonds and a suggested four-center electron-pair tetrairon molecular orbital to account for a weak bonding among the four iron atoms.

However, in the $[AsPh_4]^+[Fe_4(NO)_7(\mu_3\text{-}S)_3]^-$ structure no changes in the Fe–NO and N–O bond lengths are observed between the Fe_A and Fe_B atoms. The Fe_A–NO bond length of 1.64 (1) Å is identical with the mean for the six Fe_B–NO

Table I. Atomic Parameters for $[AsPh_4]^+[Fe_4(NO)_7(\mu_3\text{-}S)_3]^-$ [a,b]

Atom	x	y	z	$10^5\beta_{11}$	$10^5\beta_{22}$	$10^5\beta_{33}$	$10^5\beta_{12}$	$10^5\beta_{13}$	$10^5\beta_{23}$
Fe(1)	0.9833 (1)	0.7063 (1)	1.0009 (1)	508	474	999	−102	−9	137
Fe(2)	0.9935 (1)	0.8641 (1)	1.1950 (2)	541	570	978	−18	−18	64
Fe(3)	0.9153 (1)	0.8509 (1)	0.8242 (2)	650	650	851	−225	−48	221
Fe(4)	0.7725 (1)	0.7708 (1)	1.0432 (2)	508	491	1111	−150	32	144
S(1)	1.0589 (2)	0.8260 (2)	0.9861 (3)	554	684	1043	−240	22	174
S(2)	0.9174 (2)	0.7401 (2)	1.2038 (3)	618	643	1031	−222	−44	231
S(3)	0.8453 (2)	0.7221 (2)	0.8389 (3)	664	620	962	−240	−72	58
N(1)	1.0682 (7)	0.5915 (6)	0.9790 (9)	647	544	1529	−109	−68	176
N(2-1)	0.8991 (7)	0.9731 (6)	1.2099 (9)	756	498	1547	−287	109	−15
N(2-2)	1.0972 (7)	0.8543 (7)	1.3145 (9)	757	933	1080	−378	190	−56
N(3-1)	0.9667 (8)	0.8269 (7)	0.6759 (10)	862	1111	1061	−432	−46	140
N(3-2)	0.8230 (7)	0.9613 (6)	0.8459 (9)	606	636	1424	−214	−80	345
N(4-1)	0.7016 (7)	0.6949 (6)	1.0651 (8)	656	656	1149	−244	−112	352
N(4-2)	0.7008 (7)	0.8912 (6)	1.0416 (9)	616	635	1226	−207	192	152
O(1)	1.1240 (7)	0.5080 (6)	0.9592 (11)	1040	543	3664	34	271	−19
O(2-1)	0.8395 (7)	1.0536 (6)	1.2369 (10)	1111	672	3186	−121	282	173
O(2-2)	1.1606 (7)	0.8708 (7)	1.4097 (8)	992	1616	1255	−691	−120	−93
O(3-1)	0.9900 (8)	0.8314 (8)	0.5661 (9)	1661	2003	1251	−665	282	402
O(3-2)	0.7578 (7)	1.0404 (6)	0.8355 (9)	951	813	2383	−125	122	587
O(4-1)	0.6354 (7)	0.6597 (6)	1.0856 (8)	1008	1000	1649	−595	16	244
O(4-2)	0.6324 (7)	0.9690 (6)	1.0282 (9)	972	685	2160	156	297	353
As	0.5674 (1)	0.6909 (1)	0.4634 (1)	478	478	976	−113	−72	206

	x	y	z	B, Å²		x	y	z	B, Å²
C(1-1)	0.4880 (8)	0.7238 (7)	0.6222 (10)	3.2	H(1-2)	0.5973	0.7830	0.7470	6.0[c]
C(1-2)	0.5290 (9)	0.7698 (8)	0.7465 (12)	4.2	H(1-3)	0.4936	0.8307	0.9468	6.0
C(1-3)	0.4673 (9)	0.7958 (8)	0.8585 (12)	4.7	H(1-4)	0.3272	0.7985	0.9292	6.0
C(1-4)	0.3694 (10)	0.7780 (8)	0.8463 (12)	4.9	H(1-5)	0.2592	0.7168	0.7245	6.0
C(1-5)	0.3303 (9)	0.7314 (8)	0.7293 (12)	4.8	H(1-6)	0.3614	0.6704	0.5260	6.0
C(1-6)	0.3905 (8)	0.7033 (7)	0.6147 (11)	3.9	H(2-2)	0.6655	0.5494	0.6750	6.0
C(2-1)	0.7000 (8)	0.5863 (7)	0.4933 (10)	3.3	H(2-3)	0.8298	0.4112	0.7005	6.0
C(2-2)	0.7191 (9)	0.5322 (8)	0.6047 (11)	4.6	H(2-4)	0.9548	0.3720	0.5375	6.0
C(2-3)	0.8152 (10)	0.4526 (9)	0.6209 (13)	5.8	H(2-5)	0.9252	0.4696	0.3487	6.0
C(2-4)	0.8873 (11)	0.4302 (9)	0.5260 (14)	6.5	H(2-6)	0.7621	0.6043	0.3200	6.0
C(2-5)	0.8696 (10)	0.4849 (9)	0.4160 (13)	6.1	H(3-2)	0.4615	0.8592	0.2894	6.0
C(2-6)	0.7761 (9)	0.5647 (8)	0.4016 (12)	4.8	H(3-3)	0.4981	1.0105	0.2544	6.0
C(3-1)	0.5979 (8)	0.8094 (7)	0.4259 (10)	3.5	H(3-4)	0.6556	1.0482	0.3652	6.0
C(3-2)	0.5279 (9)	0.8756 (8)	0.3388 (11)	4.4	H(3-5)	0.7762	0.9388	0.5140	6.0
C(3-3)	0.5500 (9)	0.9625 (8)	0.3164 (12)	4.7	H(3-6)	0.7410	0.7835	0.5565	6.0
C(3-4)	0.6396 (9)	0.9854 (8)	0.3827 (11)	4.5	H(4-2)	0.5892	0.4965	0.2887	6.0
C(3-5)	0.7104 (10)	0.9204 (9)	0.4672 (12)	5.5	H(4-3)	0.4780	0.4316	0.1038	6.0
C(3-6)	0.6902 (9)	0.8311 (8)	0.4933 (12)	5.1	H(4-4)	0.3133	0.5387	0.0203	6.0
C(4-1)	0.4806 (8)	0.6412 (7)	0.3121 (10)	3.1	H(4-5)	0.2461	0.7087	0.1192	6.0
C(4-2)	0.5172 (8)	0.5416 (7)	0.2535 (10)	3.5	H(4-6)	0.3563	0.7759	0.3123	6.0
C(4-3)	0.4537 (8)	0.5040 (7)	0.1463 (11)	3.9					
C(4-4)	0.3562 (9)	0.5670 (8)	0.1006 (12)	4.9					
C(4-5)	0.3189 (9)	0.6654 (8)	0.1542 (12)	5.0					
C(4-6)	0.3808 (8)	0.7042 (7)	0.2683 (10)	3.9					

[a] Estimated standard deviation of last significant figures are given in parentheses. [b] Anisotropic thermal parameters of the form $\exp[-(\beta_{11}h^2 + \beta_{22}k^2 + \beta_{33}l^2 + 2\beta_{12}hk + 2\beta_{13}hl + 2\beta_{23}kl)]$ were used. [c] Hydrogen atoms were assigned fixed isotropic thermal factors of 6.0 Å².

bond lengths (of range 1.63 (1)–1.65 (1) Å). The apical N–O bond length of 1.17 (1) Å is analogous to the mean of 1.18 Å for the six basal N–O bond lengths (of range 1.17 (1)–1.20 (1) Å). Hence, there is no bond-length indication of greater $d\pi(Fe) \rightarrow \pi^*(NO)$ back-bonding in the Fe_A–NO bond than in the Fe_B–NO bonds even though this expected electronic variation is in harmony with the interpretation of the Mössbauer data on the monohydrated cesium salt.

(c) Stereochemical Relationship with $Fe_2(NO)_4(\mu_2\text{-}SC_2H_5)_2$ and $Fe_4(NO)_4(\mu_3\text{-}S)_4$. A comparison of the geometry of the $[Fe_4(NO)_7(\mu_3\text{-}S)_3]^-$ monoanion with those of the red ethyl ester,[18] $Fe_2(NO)_4(\mu_2\text{-}SC_2H_5)_2$, and of the $Fe_4(NO)_4(\mu_3\text{-}S)_4$ molecule[1,2] is particularly informative in that the localized bonding environment about each Fe_B (viz., two terminal nitrosyl ligands, two bridging sulfur atoms, and the Fe_A atom) approximates that about each of the two equivalent iron atoms in the $Fe_2(NO)_4(\mu_2\text{-}SC_2H_5)_2$ molecule, while the localized bonding environment about Fe_A (viz., one terminal nitrosyl ligand, three bridging sulfur atoms, and three Fe_B atoms) is similar to that about each of the four equivalent iron atoms in the cubic T_d $Fe_4(NO)_4(\mu_3\text{-}S)_4$.

In this context, the monoanion may be considered as a construct of three molecules of $Fe_2(NO)_4(\mu_2\text{-}SC_2H_5)_2$, without the ethyl groups (corresponding to the red $[Fe_2(NO)_4(\mu_2\text{-}S)_2]^{2-}$ dianion[17]) and minus an NO at one of the two iron atoms, fused at the common Fe(NO) point so as to share adjacent Fe–S edges. This construct emphasizes the unusually close structural similarity found between the corresponding fragments of their geometries.

The framework of the $[Fe_4(NO)_7(\mu_3\text{-}S)_3]^-$ monoanion may likewise be visualized as arising from $Fe_4(NO)_4(\mu_3\text{-}S)_4$ by the formal removal of one sulfur atom together with the addition both of a nitrosyl ligand to each of the three basal Fe–Fe bonds and of one electron to form the monoanion. The concomitant breakage of the three basal Fe–Fe electron-pair bonds in $Fe_4(NO)_4(\mu_3\text{-}S)_4$ in the above formal construction of the monoanion is a consequence of the resulting electronic structure involving a net addition of six electrons to the corresponding antibonding combinations of these basal triiron symmetry orbitals (i.e., in $Fe_4(NO)_4(\mu_3\text{-}S)_4$ only the bonding combinations are completely occupied to give a completely bonding iron tetrahedron[1,2]) such that a so-called closed-shell

Table II. Interatomic Distances and Bond Angles for $[AsPh_4]^+[Fe_4(NO)_7(\mu_3\text{-}S)_3]^-$

A. Intraanion Distances,[a] A

Fe(1)-Fe(2)	2.708 (2)	Fe(1)-N(1)	1.64 (1)
Fe(1)-Fe(3)	2.708 (2)	Fe(2)-N(2-1)	1.63 (1)
Fe(1)-Fe(4)	2.683 (2)	Fe(3)-N(3-1)	1.63 (1)
	2.700 (av)	Fe(4)-N(4-1)	1.65 (1)
Fe(2)···Fe(3)	3.628 (2)		1.64 (av)
Fe(2)···Fe(4)	3.564 (2)	Fe(2)-N(2-2)	1.65 (1)
Fe(3)···Fe(4)	3.519 (2)	Fe(3)-N(3-2)	1.64 (1)
	3.570 (av)	Fe(4)-N(4-2)	1.65 (1)
Fe(1)-S(1)	2.209 (3)		1.65 (av)
Fe(1)-S(2)	2.205 (3)	N(1)-O(1)	1.17 (1)
Fe(1)-S(3)	2.205 (3)	N(2-1)-O(2-1)	1.17 (1)
	2.206 (av)	N(3-1)-O(3-1)	1.17 (1)
Fe(2)-S(1)	2.255 (3)	N(4-1)-O(4-1)	1.17 (1)
Fe(2)-S(2)	2.254 (3)		1.17 (av)
Fe(3)-S(1)	2.251 (3)		
Fe(3)-S(3)	2.274 (3)	N(2-2)-O(2-2)	1.20 (1)
Fe(4)-S(2)	2.257 (3)	N(3-2)-O(3-2)	1.17 (1)
Fe(4)-S(3)	2.258 (3)	N(4-2)-O(4-2)	1.18 (1)
	2.258 (av)		1.18 (av)
S(1)···S(2)	3.545 (4)		
S(1)···S(3)	3.561 (4)		
S(2)···S(3)	3.555 (4)		
	3.554 (av)		

B. Intracation Distances, A

As-C(1-1)	1.91 (1)	C(3-1)-C(3-2)	1.38 (1)
As-C(2-1)	1.90 (1)	C(3-2)-C(3-3)	1.38 (1)
As-C(3-1)	1.90 (1)	C(3-3)-C(3-4)	1.36 (1)
As-C(4-1)	1.91 (1)	C(3-4)-C(3-5)	1.36 (1)
C(1-1)-C(1-2)	1.41 (1)	C(3-5)-C(3-6)	1.41 (1)
C(1-2)-C(1-3)	1.40 (1)	C(3-6)-C(3-1)	1.38 (1)
C(1-3)-C(1-4)	1.36 (1)	C(4-1)-C(4-2)	1.38 (1)
C(1-4)-C(1-5)	1.35 (1)	C(4-2)-C(4-3)	1.38 (1)
C(1-5)-C(1-6)	1.37 (1)	C(4-3)-C(4-4)	1.36 (1)
C(1-6)-C(1-1)	1.40 (1)	C(4-4)-C(4-5)	1.36 (1)
C(2-1)-C(2-2)	1.37 (1)	C(4-5)-C(4-6)	1.42 (1)
C(2-2)-C(2-3)	1.40 (1)	C(4-6)-C(4-1)	1.38 (1)
C(2-3)-C(2-4)	1.35 (1)		
C(2-4)-C(2-5)	1.36 (2)		
C(2-5)-C(2-6)	1.36 (1)		
C(2-6)-C(2-1)	1.38 (2)		

C. Intraanion Bond Angles,[a] Deg

Fe(2)-Fe(1)-Fe(3)	84.2 (1)	Fe(2)-S(1)-Fe(3)	107.2 (1)
Fe(2)-Fe(1)-Fe(4)	82.8 (1)	Fe(2)-S(2)-Fe(4)	104.4 (1)
Fe(3)-Fe(1)-Fe(4)	81.5 (1)	Fe(3)-S(3)-Fe(4)	101.9 (1)
	82.8 (av)		105.2 (av)
S(1)-Fe(1)-Fe(2)	53.4 (1)	S(1)-Fe(1)-S(2)	106.9 (1)
S(1)-Fe(1)-Fe(3)	53.3 (1)	S(1)-Fe(1)-S(3)	107.3 (1)
S(2)-Fe(1)-Fe(2)	53.4 (1)	S(2)-Fe(1)-S(3)	107.7 (1)
S(2)-Fe(1)-Fe(4)	53.9 (1)		108.0 (av)
S(3)-Fe(1)-Fe(3)	54.0 (1)		
S(3)-Fe(1)-Fe(4)	54.0 (1)	S(1)-Fe(2)-S(2)	103.7 (1)
	53.7 (av)	S(1)-Fe(3)-S(3)	103.5 (1)
		S(2)-Fe(4)-S(3)	104.1 (1)
S(1)-Fe(2)-Fe(1)	51.9 (1)		103.8 (av)
S(1)-Fe(3)-Fe(1)	51.9 (1)		
S(2)-Fe(2)-Fe(1)	51.8 (1)	N(1)-Fe(1)-Fe(2)	130.0 (3)
S(2)-Fe(4)-Fe(1)	52.2 (1)	N(1)-Fe(1)-Fe(3)	129.1 (3)
S(3)-Fe(3)-Fe(1)	51.6 (1)	N(1)-Fe(1)-Fe(4)	131.6 (3)
S(3)-Fe(4)-Fe(1)	52.2 (1)		130.2 (av)
	52.3 (av)		
Fe(1)-S(1)-Fe(2)	74.7 (1)	N(2-1)-Fe(2)-Fe(1)	124.8 (3)
Fe(1)-S(1)-Fe(3)	74.8 (1)	N(3-1)-Fe(3)-Fe(1)	118.2 (3)
Fe(1)-S(2)-Fe(2)	74.8 (1)	N(4-1)-Fe(4)-Fe(1)	124.0 (3)
Fe(1)-S(2)-Fe(4)	73.9 (1)		122.3 (av)
Fe(1)-S(3)-Fe(3)	74.4 (1)		
Fe(1)-S(3)-Fe(4)	73.9 (1)	N(2-2)-Fe(2)-Fe(1)	121.0 (3)
	74.4 (av)	N(3-2)-Fe(3)-Fe(1)	127.3 (3)
		N(4-2)-Fe(4)-Fe(1)	121.9 (3)
N(1)-Fe(1)-S(1)	112.5 (3)		123.4 (av)
N(1)-Fe(1)-S(2)	112.6 (3)		
N(1)-Fe(1)-S(3)	109.6 (3)	N(2-1)-Fe(2)-N(2-2)	114.2 (4)
	111.6 (av)	N(3-1)-Fe(3)-N(3-2)	114.5 (5)
		N(4-1)-Fe(4)-N(4-2)	114.0 (4)
N(2-1)-Fe(2)-S(1)	113.2 (3)		114.2 (av)
N(2-1)-Fe(2)-S(2)	108.1 (3)		
N(3-1)-Fe(3)-S(1)	105.3 (3)	Fe(1)-N(1)-O(1)	176.3 (9)
N(3-1)-Fe(3)-S(3)	106.7 (3)	Fe(2)-N(2-1)-O(2-1)	171.0 (9)
N(4-1)-Fe(4)-S(2)	106.2 (3)	Fe(3)-N(3-1)-O(3-1)	165.1 (10)
N(4-1)-Fe(4)-S(3)	110.0 (3)	Fe(4)-N(4-1)-O(4-1)	166.3 (8)
	108.2 (av)		167.5 (av)
N(2-2)-Fe(2)-S(1)	107.8 (3)		
N(2-2)-Fe(2)-S(2)	109.4 (3)	Fe(2)-N(2-2)-O(2-2)	164.6 (9)
N(3-2)-Fe(3)-S(1)	115.2 (3)	Fe(3)-N(3-2)-O(3-2)	167.5 (9)
N(3-2)-Fe(3)-S(3)	110.7 (3)	Fe(4)-N(4-2)-O(4-2)	166.1 (8)
N(4-2)-Fe(4)-S(2)	115.3 (3)		166.1 (av)
N(4-2)-Fe(4)-S(3)	106.7 (3)		
	110.8 (av)		

D. Intracation Bond Angles, Deg

C(1-1)-As-C(2-1)	111.0 (4)	C(3-1)-C(3-2)-C(3-3)	120.5 (10)
C(1-1)-As-C(3-1)	109.1 (4)	C(3-2)-C(3-3)-C(3-4)	120.2 (11)
C(1-1)-As-C(4-1)	107.6 (4)	C(3-3)-C(3-4)-C(3-5)	120.0 (11)
C(2-1)-As-C(3-1)	109.3 (4)	C(3-4)-C(3-5)-C(3-6)	121.3 (11)
C(2-1)-As-C(4-1)	108.0 (4)	C(3-5)-C(3-6)-C(3-1)	117.9 (11)
C(3-1)-As-C(4-1)	111.8 (4)	C(3-6)-C(3-1)-C(3-2)	119.9 (10)
C(1-1)-C(1-2)-C(1-3)	118.3 (10)	C(4-1)-C(4-2)-C(4-3)	119.8 (9)
C(1-2)-C(1-3)-C(1-4)	120.2 (11)	C(4-2)-C(4-3)-C(4-4)	118.8 (10)
C(1-3)-C(1-4)-C(1-5)	122.2 (11)	C(4-3)-C(4-4)-C(4-5)	122.8 (11)
C(1-4)-C(1-5)-C(1-6)	119.2 (11)	C(4-4)-C(4-5)-C(4-6)	119.2 (11)
C(1-5)-C(1-6)-C(1-1)	119.9 (10)	C(4-5)-C(4-6)-C(4-1)	117.8 (9)
C(1-6)-C(1-1)-C(1-2)	120.1 (9)	C(4-6)-C(4-1)-C(4-2)	121.4 (9)
C(2-1)-C(2-2)-C(2-3)	119.6 (10)		
C(2-2)-C(2-3)-C(2-4)	119.4 (12)		
C(2-3)-C(2-4)-C(2-5)	121.3 (13)		
C(2-4)-C(2-5)-C(2-6)	119.2 (12)		
C(2-5)-C(2-6)-C(2-1)	120.5 (11)		
C(2-6)-C(2-1)-C(2-2)	119.9 (10)		

[a] The distances and bond angles of the $[Fe_4(NO)_7(\mu_3\text{-}S)_3]^-$ anion were averaged in accord with an idealized C_{3v} geometry.

electronic configuration is maintained about each iron atom.

The close compliance of the dimensions in the $(ON)_2Fe_BS_2Fe_A$ fragment of the monoanion with those in the $Fe_2(NO)_2(\mu_2\text{-}SC_2H_5)_2$ molecule[18] is seen from the following comparison of corresponding means: (1) the Fe_B–S bond length of 2.26 vs. 2.27 Å; (2) the Fe_B–NO and N–O bond lengths of 1.64 vs. 1.67 Å and 1.18 vs. 1.17 Å, respectively; and (3) the ON–Fe_B–NO and S–Fe_B–S bond angles of 114 vs. 117° and 104 vs. 106°, respectively.

The similarity in the dimensions of the $(ON)Fe_AS_3(Fe_B)_3$ fragment in the monoanion with those in the $Fe_4(NO)_4(\mu_3\text{-}S)_4$ molecule is disclosed from the following comparison of cor-

responding means: (1) the Fe_A–S bond length of 2.21 vs. 2.22 Å; (2) the Fe_A–NO and N–O bond lengths of 1.64 vs. 1.66 Å and 1.17 vs. 1.16 Å, respectively; and (3) the ON–Fe_A–S and S–Fe_A–S bond angles of 112 vs. 114° and 108 vs. 104°.

The above comparisons of the mean molecular dimensions parallel the trend that the Fe_A–S bonds are 0.05 Å shorter than the Fe_B–S bonds in the three chemically equivalent $Fe_AS_2Fe_B$ fragments in the monoanion. Furthermore, the bonding Fe_A–Fe_B distance of 2.70 Å is between that of 2.65 Å in $Fe_4(NO)_4(\mu_3\text{-}S)_4$ and 2.72 Å in $Fe_2(NO)_4(\mu_2\text{-}SC_2H_5)_2$ in accord with each $Fe_AS_2Fe_B$ fragment being considered as a composite of a Fe_AS_2-type fragment from $Fe_4(NO)_4(\mu_3\text{-}S)_4$ and a Fe_BS_2-type fragment from $Fe_2(NO)_4(\mu_2\text{-}SC_2H_5)_2$.

In contrast to the near linearity (176 (1)°) of the Fe_A–N–O bond angle in the monoanion, the two kinds of Fe_B–N–O bond angles (under assumed C_{3v} symmetry) both show pronounced deviations from linearity with similar ranges of 165 (1)–168 (1)° and 165 (1)–171 (1)°. An analogous Fe–N–O bond-angle trend is observed in $Fe_4(NO)_4(\mu_3\text{-}S)_4$ compared to $Fe_2(NO)_2(\mu_2\text{-}SC_2H_5)_2$ with a near-linear range of 176.9 (5)–178.8 (5)° in the former molecule containing four chemically equivalent $S_3Fe_A(NO)$-type fragments (of localized C_{3v} symmetry) in contrast to a 167.2 (±3.5)–167.7 (±3.5)° range in the latter molecule containing two crystallographically equivalent $S_2Fe_B(NO)_2$-type fragments (of localized C_{2v} symmetry). The significantly greater deviations of the Fe–N–O bond angles from 180° in the iron dinitrosyl fragments may be readily attributed to electronic effects (superimposed on crystal packing effects), first suggested by Kettle[27] for M–C–O bonds in metal carbonyl complexes and subsequently utilized by Enemark[28] to rationalize solid-state distortions in mononuclear metal nitrosyl complexes. These electronic arguments[27,28] assume that the number of ligands attached to the metal and the localized symmetry for the metal are important in determining an Fe–N–O bond angle. Whenever the symmetry at the metal is lower than C_3, then the two π^* orbitals of the NO ligand will no longer be degenerate. The equilibrium geometry of the NO group in the molecule will then depend upon the interplay of $d\pi(M) \rightarrow \pi^*(NO)$ bonding and (metal)electron–(ligand)electron repulsion.

(d) Resulting Bonding Implications. The close conformity in dimensions of each (Fe–Fe)-bonding $Fe_AS_2Fe_B$ fragment in the monoanion to both the six (Fe–Fe)-bonding $Fe_AS_2Fe_A$ fragments in $Fe_4(NO)_4(\mu_3\text{-}S)_4$ and the one (Fe–Fe)-bonding $Fe_BS_2Fe_B$ fragment in $Fe_2(NO)_4(\mu_2\text{-}SC_2H_5)_2$ is also apparent from the sharply acute Fe–S–Fe bond angles of range 73.9 (1)–74.8 (1)° and mean 74.4° in the three $Fe_AS_2Fe_B$ fragments of the monoanion being essentially identical with the corresponding bond angles of 73.1 (1)° in $Fe_2(NO)_4(\mu_2\text{-}SC_2H_5)_2$ and of range 73.0 (5)–73.9 (5)° and mean 73.4° in $Fe_4(NO)_4(\mu_3\text{-}S)_4$. This essential invariance in the angular dimensions of the Fe–Fe bonding Fe_2S_2 bridging systems in the above three related complexes indicates that the nature of the Fe–Fe interaction in each Fe_2S_2 fragment must be similar.

A qualitative formulation of the electron-pair coupling interaction between the iron atoms in the diamagnetic $Fe_2(NO)_4(\mu_2\text{-}SC_2H_5)_2$ complex as a direct electron-pair σ bond was put forth by Dahl, Rodulfo de Gil, and Feltham[29] from their structural investigation of the electronically equivalent and structurally analogous $Fe_2(NO)_4(\mu_2\text{-}I)_2$ molecule in order to rationalize the different kind and degree of polymerization of $Fe(NO)_2I$ and $Co(NO)_2I$ in their respective solid-state structures. Their model assumes that the five valence d atomic orbitals of each d^9 Fe(–I) can be classified, by linear combination, into 18 localized diiron symmetry orbitals of which, from overlap considerations, the antibonding σ^* level is assumed to be the highest energy unoccupied orbital, thereby resulting in a net electron-pair Fe–Fe σ bond. A qualitative molecular orbital model, invoked[2] to describe the tetrairon bonding in the $Fe_4(NO)_4(\mu_3\text{-}S)_4$ molecule, considers the 3d atomic orbital interactions of four d^7 Fe(I) (arising by virtue of the coordination of each iron atom with one terminal NO^+ and three triply bridging S^{2-} ligands). The resulting placement of the 28 valence d electrons from the four iron atoms into the 20 tetrairon symmetry combinations under T_d symmetry produces an electronic configuration involving 12 electrons completely occupying six strongly bonding ($a_1 + e + t_2$) tetrairon levels, with no electrons in the corresponding antibonding ($t_1 + t_2$) tetrairon level. This delocalized metal cluster description is conceptually equivalent, under a localized valence bond representation, to each of the six Fe_2S_2 fragments possessing an electron-pair bond which is directed along one of the six edges of the completely bonding iron tetrahedron.

These Fe–Fe bonding models for $Fe_2(NO)_6(\mu_2\text{-}SC_2H_5)_2$ and $Fe_4(NO)_4(\mu_3\text{-}S)_4$ suggest that the Fe–Fe bonding in the $[Fe_4(NO)_7(\mu_3\text{-}S)_3]^-$ monoanion can be analogously described under C_{3v} symmetry as arising from the 3d AO interactions of an apical d^7 Fe(I) with three basal d^9 Fe(–I) such that the 34 valence d electrons available from the four iron atoms occupy 17 of the 20 tetrairon cluster orbitals (constructed from the five 3d AO's of each of the four irons). It follows that there is a net stabilization from the bonding Fe–Fe interactions of three occupied ($a_1 + e$) tetrairon levels (for which the corresponding antibonding levels are empty), which can be decomposed under a localized valence bond representation into an electron-pair Fe–Fe bond in each of the three $Fe_AS_2Fe_B$ systems.

Acknowledgment. We are happy to acknowledge the financial support rendered by the National Science Foundation (No. GP-42309X) for this investigation. The use of the UNIVAC 1110 computer at the Academic Computing Center, University of Wisconsin–Madison, was made available through partial support of the National Science Foundation, administered through the University Research Committee. Special thanks are given to Mr. John Compton and Mr. John Collier at the University of Wisconsin—Madison for their assistance in computing.

Supplementary Material Available: Table III containing equations of least-squares planes along with perpendicular displacements of atoms and interplanar angles and Table IV containing observed and calculated structure factors (16 pages). Ordering information is given on any current masthead page.

Registry No. $[AsPh_4]^+[Fe_4(NO)_7(\mu_3\text{-}S)_3]^-$, 63704-10-9; $Fe_4(NO)_4(\mu_3\text{-}S)_4$, 53276-80-5; $Fe_2(NO)_4(\mu_2\text{-}SC_2H_5)_2$, 15020-36-7.

References and Notes

(1) (a) C. Ting-Wah Chu, Ph.D. Thesis, University of Wisconsin—Madison, 1977; (b) R. S. Gall, Ph.D. Thesis, University of Wisconsin—Madison, 1973.
(2) R. S. Gall, C. Ting-Wah Chu, and L. F. Dahl, *J. Am. Chem. Soc.*, **96**, 4019 (1974).
(3) (a) Trinh-Toan, Ph.D. Thesis, University of Wisconsin—Madison, 1972; (b) B. K. Teo, Ph.D. Thesis, University of Wisconsin—Madison, 1973; (c) L. F. Dahl, Abstracts of Papers, 165th National Meeting of the American Chemical Society, Dallas, Texas, April 1973, INOR 6; (d) L. F. Dahl, J. D. Sinclair, and B. K. Teo in "The Organic Chemistry of Iron", E. A. Koerner von Gustorf, Ed., Academic Press, New York, N.Y. 1977; (e) B. K. Teo, Trinh-Toan, and L. F. Dahl, to be submitted for publication.
(4) (a) R. A. Schunn, C. J. Fritchie, Jr., and C. T. Prewitt, *Inorg. Chem.*, **5**, 892 (1966); (b) C. H. Wei, G. R. Wilkes, P. M. Treichel, and L. F. Dahl, *ibid.*, **5**, 900 (1966).
(5) Trinh-Toan, W. P. Fehlhammer, and L. F. Dahl, *J. Am. Chem. Soc.*, **99**, 402 (1977).
(6) Trinh-Toan, B. K. Teo, J. A. Ferguson, T. J. Meyer, and L. F. Dahl, *J. Am. Chem. Soc.*, **99**, 408 (1977).
(7) (a) T. Herskovitz, B. A. Averill, R. H. Holm, J. A. Ibers, W. D. Phillips, and J. F. Weiher, *Proc. Natl. Acad. Sci. U.S.A.*, **69**, 2437 (1972); (b) B. A. Averill, T. Herskovitz, R. H. Holm, and J. A. Ibers, *J. Am. Chem. Soc.*, **95**, 3423 (1973); (c) L. Que, Jr., M. A. Bobrik, J. A. Ibers, and R. H. Holm, *ibid.*, **96**, 4168 (1974).
(8) G. Johansson and W. N. Lipscomb, *Acta Crystallogr.*, **11**, 594 (1958); *J. Chem. Phys.*, **27**, 1417 (1957).

(9) R. B. King, "Organometallic Syntheses", Vol. 1, Academic Press, New York, N.Y., 1965, p 149.
(10) An x-ray diffraction examination of the black crystals obtained from the acetone–ether mixture indicated a different crystalline form of orthorhombic symmetry. A subsequent high-resolution infrared spectrum (Digilab Fts-20 spectrometer) of the crystalline sample (KBr pellet) showed a different infrared spectrum characteristic of the sought-after $[AsPh_4]^+[Fe_4(NO)_4(\mu_3\text{-}S)_4]^-$ salt. This compound is under further structural investigation.
(11) (a) J. C. Calabrese, FOBS, a Fortran diffractometer data reduction program, University of Wisconsin—Madison, 1972; (b) J. C. Calabrese, SORTMERGE, Ph.D. Thesis (Appendix I), University of Wisconsin—Madison, 1971, a Fortran program for the merging and decay correction of data; (c) J. F. Blount, DEAR, a Fortran absorption correction program based on the method given by W. R. Busing and H. A. Levy, *Acta Crystallogr.*, **10**, 180 (1957); (d) J. C. Calabrese, MAP, a local Fortran Fourier summation and molecular assemblage program, 1972; (e) J. C. Calabrese, PHASE, Ph.D. Thesis (Appendix II), University of Wisconsin—Madison, 1971; (f) J. C. Calabrese, MIRAGE, Ph.D. Thesis (Appendix III), University of Wisconsin—Madison, 1971; (g) J. C. Calabrese, "A Crystallographic Variable Matrix Least-Squares Refinement Program", University of Wisconsin—Madison, 1972; (h) W. R. Busing, K. O. Martin, and H. A. Levy, "ORFLS, A Fortran Crystallographic Least-Squares Program", ORNL-TM-305, Oak Ridge National Laboratory, Oak Ridge, Tenn., 1962; (i) W. R. Busing, K. O. Martin, and H. A. Levy, "ORFFE, A Fortran Crystallographic Function and Error Program", ORNL-TM-306, Oak Ridge National Laboratory, Oak Ridge, Tenn., 1962; (j) D. L. Smith, PLANES, Ph.D. Thesis (Appendix IV), University of Wisconsin—Madison, 1962; (k) C. K. Johnson, "ORTEP, A Fortran Thermal Ellipsoid Plot Program for Crystal Structure Illustration", ORNL-3794, Oak Ridge National Laboratory, Oak Ridge, Tenn., 1964.
(12) "International Tables for X-Ray Crystallography", Vol. III, Kynoch Press, Birmingham, England, 1968, (a) p 162; (b) p 215.
(13) $R_1 = [\sum||F_o| - |F_c||/\sum|F_o|] \times 100$ and $R_2 = [\sum w_i||F_o| - |F_c||^2/\sum w_i|F_o|^2]^{1/2} \times 100$. All least-squares refinements were based on the minimization of $\sum w_i||F_o| - |F_c||^2$ with the individual weights $w_i = 1/\sigma(|F_o|)^2$. The standard deviation of an observation of unit weight σ_1, is defined by $[\sum w_i|F_o^2 - F_c^2|/(n-p)]^{1/2}$ where σ_c is determined by counting statistics and where n denotes the number of observations and p the number of parameters varied during the least-squares refinement. For appropriately weighted data and normally distributed errors the expected value of σ_1 is unity.
(14) The scattering factor tables used for all nonhydrogen atoms are those of Cromer and Mann,[15] while those for the hydrogen atoms are from Stewart et al.[16] Real and imaginary corrections for anomalous dispersion (viz., $\Delta f' = 0.1$, $\Delta f'' 2.2$ for As; $\Delta f' = 0.4$, $\Delta f'' = 1.0$ for Fe; $\Delta f' = 0.1$, $\Delta f'' = 0.2$ for S)[12b] were included in the structure factor calculations.
(15) D. T. Cromer and J. B. Mann, *Acta Crystallogr., Sect. A.* **24**, 321 (1968).
(16) R. F. Stewart, E. R. Davidson, and W. T. Simpson, *J. Chem. Phys.*, **42**, 3175 (1965).
(17) The dimeric formulation of $K_2[Fe_2(NO)_4(\mu_2\text{-}S)_2]$ with bridging sulfur atoms is based upon the crystal and molecular structure[18] of the electronically equivalent red ethyl ester, $Fe_2(NO)_4(\mu_2\text{-}SC_2H_5)_2$.
(18) J. T. Thomas, J. H. Robertson, and E. G. Cox, *Acta Crystallogr.*, **11**, 599 (1958).
(19) M. L. Roussin, *Ann. Chim. Phys.*, **52**, 285 (1958).
(20) (a) O. Pavel, *Ber.*, **15**, 2600 (1882); (b) K. A. Hofmann and O. F. Wiede, *Z. Anorg. Allg. Chem.*, **9**, 295 (1895).
(21) C. C. Addison and J. Lewis, *Q. Rev. Chem. Soc.*, **9**, 115 (1955).
(22) W. Manchot and E. Linckh, *Ber.*, **59**, 412 (1926).
(23) F. Seel, *Z. Anorg. Allg. Chem.*, **249**, 308 (1942).
(24) L. Cambi and L. Szegö, *Atti R. Acad. Naz. Lincei, Cl. Sci. Fiz., Mat. Nat.*, **13**, 168 (1931).
(25) W. Kerler, W. Neuwirth, E. Fluck, P. Kuhn, and B. Zimmermann, *Z. Phys.*, **173**, 321 (1963).
(26) E. Kostiner, J. Steger, and J. R. Rea, *Inorg. Chem.*, **9**, 1939 (1970).
(27) S. F A. Kettle, *Inorg. Chem.*, **4**, 1661 (1965).
(28) (a) J. H. Enemark, *Inorg. Chem.*, **10**, 1952 (1971); (b) J. H. Enemark and R. D. Feltham, *Coord. Chem. Rev.*, **13**, 339 (1974).
(29) L. F. Dahl, E. Rodulfo de Gil, and R. D. Feltham, *J. Am. Chem. Soc.*, **91**, 1653 (1969).

Contribution from the Department of Chemistry, University of Virginia, Charlottesville, Virginia 22901

Crystal and Molecular Structure of 5-(η^5-C_5H_5)CoB_9H_{13}, a Cobaltaborane Analogue of $B_{10}H_{14}$

J. ROBERT PIPAL and RUSSELL N. GRIMES*

Received April 13, 1977 AIC70267W

The structure of 5-(η^5-cyclopentadienyl)-5-cobalta-*nido*-decaborane(14) was determined from a single-crystal x-ray diffraction investigation. The molecule consists of a $B_{10}H_{14}$-like cage in which a (η^5-C_5H_5)Co group replaces a BH unit at the 5 position, in agreement with the structure originally proposed from ^{11}B and ^1H NMR spectra. The compound crystallizes in the monoclinic space group $P2_1/c$, with $a = 8.649$ (3) Å, $b = 12.826$ (6) Å, $c = 11.545$ (5) Å, $\beta = 106.90$ (3)°, $\rho_{obsd} = 1.25$ (2) g cm^{-3}, and $\rho_{calcd} = 1.28$ g cm^{-3} for $Z = 4$. The structure was refined by full-matrix least-squares methods to a final R value of 4.3% and R_w of 5.1% for the 1166 reflections for which $F_o^2 > 3\sigma(F_o^2)$. The molecule has four bridging hydrogens on the open face, of which three are of the B–H–B type and one is B–H–Co, the positions being analogous to those in $B_{10}H_{14}$. The compound is structurally related to other *nido*-metalloboranes containing an MB_9 cage and also to (η^5-C_5H_5)$CoC_2B_7H_{11}$, a *nido*-cobaltacarborane. It can also be viewed as a metal complex consisting of $B_9H_{13}^{2-}$ and η^5-$C_5H_5^-$ ligands sandwiched around a Co^{3+} ion, with the B_4 face of the borane ligand nearly parallel to the $C_5H_5^-$ plane.

Introduction

A recurring theme in metalloborane[1] and metallocarborane[2] chemistry is the formal substitution of heteroatom groups for BH or CH units in borane or carborane cage frameworks, often producing species of higher stability than the parent molecule.[3] A common replacement is that of the cyclopentadienylcobalt [(η^5-C_5H_5)Co] unit for BH; since both groups formally donate two electrons to the skeletal framework,[7] such a substitution leaves unchanged the number of electrons in skeletal bonding molecular orbitals and therefore generates no major structural alterations. An example is red crystalline 2-(η^5-C_5H_5)CoB_4H_8,[8] an analogue of B_5H_9 in which (η^5-C_5H_5)Co replaces a basal BH group. In conformity with the structure originally proposed from NMR data,[8] an x-ray investigation[9] has confirmed that the molecule retains the essential square-pyramidal shape with four basal bridging hydrogens, as in B_5H_9 itself.

The synthesis of 2-(η^5-C_5H_5)CoB_4H_8 from $B_5H_8^-$, $CoCl_2$, and $C_5H_5^-$ also gave a number of other cobaltaboranes having three or four boron atoms, but only one larger species, 5-(η^5-C_5H_5)CoB_9H_{13}, was isolated.[6b,8] This compound was characterized[6b,8] from ^{11}B and ^1H NMR spectra and the geometry proposed was that of a $B_{10}H_{14}$-like basket with the cobalt group replacing the BH in the 5 position on the open face. The present paper describes an x-ray investigation in which this structure was confirmed. Although crystallographic studies of several other cobaltaboranes from the same reaction have been conducted[10] or are in progress, (η^5-C_5H_5)CoB_9H_{13} is structurally distinct from the others and therefore is reported separately.

Experimental Section

Several red crystals of the title compound, prepared from NaB_5H_8, $CoCl_2$, and NaC_5H_5 as described elsewhere,[6b,8] were grown from a hexane solution by slow evaporation. One acicular crystal, ap-